THE JOURNAL OF PHYSICAL CHEMISTRY Letters

pubs.acs.org/JPCL

Direct Observation of the Tunneling Channels of a Chemisorbed Molecule

Benjamin W. Heinrich,[†] Cristian Iacovita,[†] Thomas Brumme,[‡,¶] Deung-Jang Choi,[†] Laurent Limot,*[,†] Mircea V. Rastei,[†] Werner A. Hofer,[§] Jens Kortus,[‡] and Jean-Pierre Bucher[†]

[†]Institut de Physique et Chimie des Matériaux de Strasbourg, UMR 7504, Université de Strasbourg, F-67034 Strasbourg, France, [‡]Institut für Theoretische Physik, TU Bergakademie Freiberg, D-09599 Freiberg, Germany, [¶]Institute for Materials Science and Max Bergmann Center of Biomaterials, Dresden University of Technology, D-01069, Dresden, Germany, and [§]Surface Science Research Centre, University of Liverpool, Liverpool L69 3BX, United Kingdom

ABSTRACT We exploit several scanning tunneling microscopy (STM) techniques, such as atom manipulated scans and constant-height scans, to atomically resolve the adsorption geometry of isolated cobalt-phthalocyanine (CoPc) molecules on a copper (111) surface and to obtain proper low-temperature maps of the molecular conductance. By comparing these crucial findings to density functional calculations, we then provide fresh insight into the CoPc−metal interface. This innovative STM study should be applicable to a wide variety of molecules relevant for molecular electronics.

SECTION Surfaces, Interfaces, Catalysis

Understanding electron transport in hybrid metal−organic devices is fundamental to the emerging technology of molecular electronics.[1] Functional molecules are in fact bound to replace diodes, transistors, and switches to answer the multiple tasks of electronic circuits. Phthalocyanine (Pc) and porphyrin derivatives have been most studied in this context, also because of their potential interest for spin-dependent electronics,[2,3] and optoelectronics.[4] The contact between a conductor and a molecule is a decisive factor for the quality of these nanoscale devices since it modifies the properties of the molecule and therefore its functionalities. For this reason, the metal−molecule contact is one of the most urgent matters to address in molecular electronics. One way to study this is to focus on model playgrounds such as single molecules adsorbed on pristine metal surfaces. Recent scanning tunneling microscopy and spectroscopy (STM and STS) studies have evidenced how the adsorption site,[5,6] the close environment,[7−9] and conformational changes,[10−12] of molecules can influence their conductance and spin-polarization.

In this letter we wish to go one step further and show how to gather crucial information on the metal−molecule interface that is usually inaccessible to STM. For this purpose we use low-temperature STM and STS to investigate a common dye molecule such as single cobalt-phthalocyanine (CoPc) on a copper (111) surface. Compared to previous studies, we exploit several innovative techniques in relation to single molecules, such as atom-manipulated scans and constant-height scans. In this way we are able to determine the adsorption site of a single CoPc and identify in a reliable way its major conductance channels with a high intramolecular resolution. By comparing these crucial parameters to density functional calculations, we are then in a favorable position to accurately describe, from a chemical viewpoint, the molecule−metal contact and to identify the origin of the conductance channels observed. This experiment may serve as an example for future investigations of single molecules at the atomic level.

The measurements were carried out with a low-temperature STM operating below 5×10^{-11} mbar. After cleaning the Cu(111) surface by argon ion bombardment and annealing, CoPc was sublimated from a crucible containing a 99.5% pure powder heated to at least 400 °C, resulting in an average coverage of 0.03 monolayers on the Cu(111) surface. A monolayer corresponds to one molecule occupying an area of 140 Å^2. The sample was then transferred in the STM and cooled to 4.6 K. STS measurements consisted in mapping the spatial variation of the differential conductance (dI/dV) at each pixel of a given area of the surface (the bias was measured with respect to the sample). The dI/dV was measured via lock-in detection by applying a modulation voltage to the bias (15 mV rms in amplitude at a frequency close to 700 Hz). During the acquisition of a dI/dV map, the feedback loop was open, and the tip was kept at a constant height relative to the copper surface. A variety of electrochemically etched W tips were employed. After a sputter/anneal cycle, the tips were treated in vacuo by soft indentations into the clean copper surface, therefore the tip apex was presumably coated with copper.

Figure 1a presents an STM image of CoPc molecules deposited on the Cu(111) surface. At this coverage, CoPc molecules are well separated from one another. This might reflect a random distribution of CoPc on the surface produced by a gas-like phase existing at room temperature, but could also be related

Received Date: March 16, 2010
Accepted Date: April 15, 2010
Published on Web Date: April 26, 2010

DOI: 10.1021/jz100346a | *J. Phys. Chem. Lett.* **2010**, *1*, 1517–1523

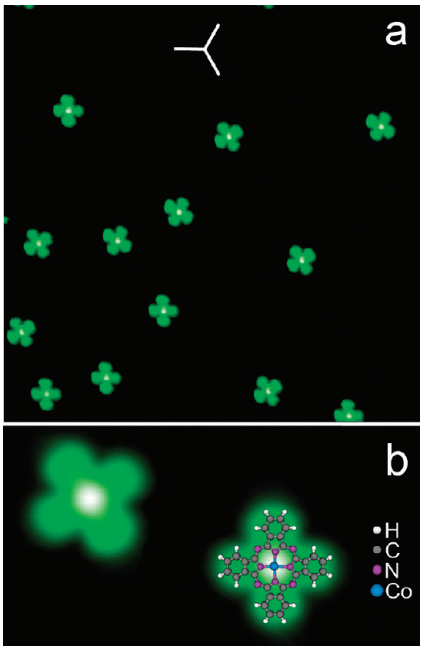

Figure 1. CoPc on Cu(111). (a) Constant-current image (size: 220 × 220 Å^2, sample bias: −1 V, tunneling current: 0.02 nA) with thick white lines indicating the three close-packed symmetry directions of the Cu(111) surface: ⟨110⟩, ⟨101⟩, and ⟨011⟩ (see also Figure 2a). (b) High-resolution constant-current image with structure model of CoPc superimposed to one molecule (40 × 21 Å^2, −1 V, 0.5 nA).

to a repulsive interaction between the molecules,[13] a higher coverage being necessary to conclude. The distribution we observe is reminiscent of what is encountered for other MPc molecules,[14,15] or even for the tetrapyridyl-porphyrin molecule.[16] In the high-resolution image of Figure 1b acquired at −1 V, the molecules have a four-lobe pattern with an apparent width of 18 Å, consistent with the known structure of the molecule. The protrusion in the center of the molecule has an apparent height of 1.6 Å and corresponds to the cobalt atom, while the four benzopyrrole groups appear as lobes with an apparent height of 1.2 Å. A careful analysis of the STM images reveals that CoPc possesses three possible azimuthal orientations on Cu(111) (thick lines in Figure 1a), which suggests that the three close-packed symmetry directions of the copper surface influence the adsorption of CoPc.

In order to determine the adsorption site of CoPc, it is necessary to image the surface atoms of the (111) lattice. This is a task that, under usual tunneling conditions, is not straightforward on compact metal surfaces because of the weak electronic corrugation. Markers such as CO molecules,[16,17] or metal atoms,[18,19] therefore need to be deposited onto the surface along with the molecules under investigation. In the present study, single copper atoms were evaported on the cold surface (Figure 2a,b) to mark the position of the hollow sites of Cu(111), either face-centered cubic (fcc) or hexagonal close packed (hcp). The evaporation was carried out through an opening of the liquid-helium shield of the cryostat by heating a degassed copper wire (> 99.99% purity) wound around a W wire. A coverage of 10 atoms for an area of 100 × 100 Å^2 was obtained with no appreciable increase

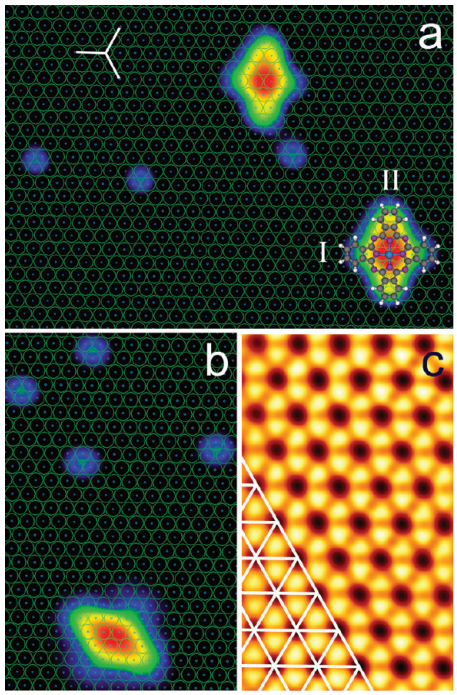

Figure 2. Unveiling the adsorption site of CoPc through tip-assisted atom manipulation. (a) Constant-current image of CoPc molecules coadsorbed with individual copper atoms (76 × 55 Å^2, −1 V, 0.05 nA) and structure model of CoPc. The (111) lattice is determined by atom manipulation (see Figure 2c, lattice constant 2.56 Å). (b) Constant-current image with the molecule adsorbed along a different close-packed symmetry direction compared to that in panel a (41 × 63 Å^2, −1 V, 0.05 nA). The copper surface was cut in the images of panels a and b for clarity (see Figure S2 of the Supporting Information for more details). (c) Manipulated atom image of the Cu(111) surface (13 × 22 Å^2, −5 mV, 15 nA). The surface lattice is indicated by white lines. The manipulated atom image can depend on the scanning angle relative to the lattice and on the tip employed, which, depending on its apex geometry, may modify the trapping potential.

of other impurities. Regardless of the marker used, this approach can prove to be very sensitive to minor miscalibrations of the piezoelement or even drift. To achieve an unambiguous determination of the lattice network without perturbing the molecule, we use the lateral manipulation of a probe atom to image the surface corrugation in close vicinity of CoPc. This operating mode of the STM consists in vertically approaching the tip toward the adsorbed atom (adatom) so to create a localized surface-potential well that traps the adatom under the tip.[20,21] Typical tunneling parameters are 5 mV for the sample bias and 10 nA or higher for the tunneling current. An image is then acquired by scanning the surface area next to the molecule with the adatom trapped beneath the tip. The "manipulated atom image" exhibits the expected C_6 symmetry of the Cu(111) surface (Figure 2c), where the height maxima correspond to fcc or hcp hollow sites (the bright triangular-like spots in Figure 2c), and the height minima (the dim spots) correspond to the position of the surface atoms. A grid representing the Cu(111) surface is extracted from Figure 2c and subsequently positioned in Figure 2a,b so that the adatoms in the images are located in a hollow position. It can then be concluded that the CoPc molecule is adsorbed in a bridge position, i.e., the cobalt atom of

DOI: 10.1021/jz100346a | J. Phys. Chem. Lett. 2010, 1, 1517–1523

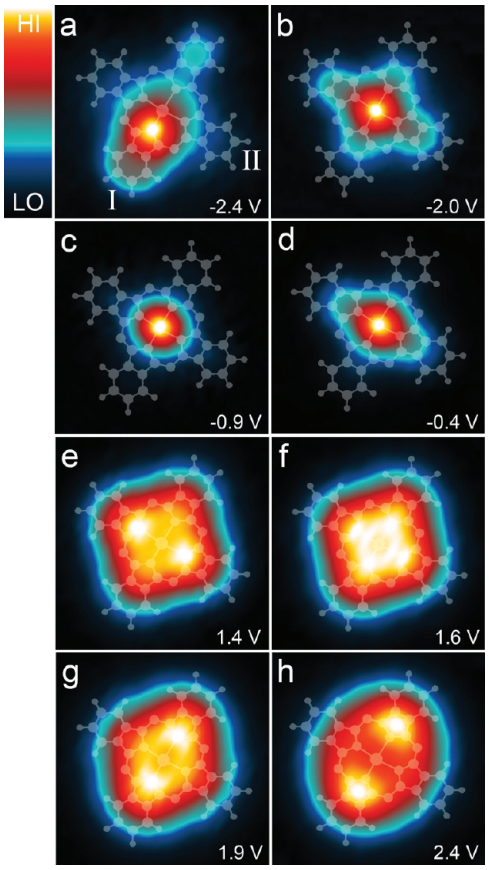

Figure 3. Constant-height dI/dV maps over CoPc (20×20 Å^2). The feedback loop was opened over Cu(111) at 0.01 nA and at a bias of (a) −2.4 V, (b) −2.0 V, (c) −0.9 V, (d) −0.4 V, (e) 1.4 V, (f) 1.6 V, (g) 1.9 V, and (h) 2.4 V. The model structure of CoPc is superimposed on the dI/dV maps in order to localize the signal maximum on the molecule.

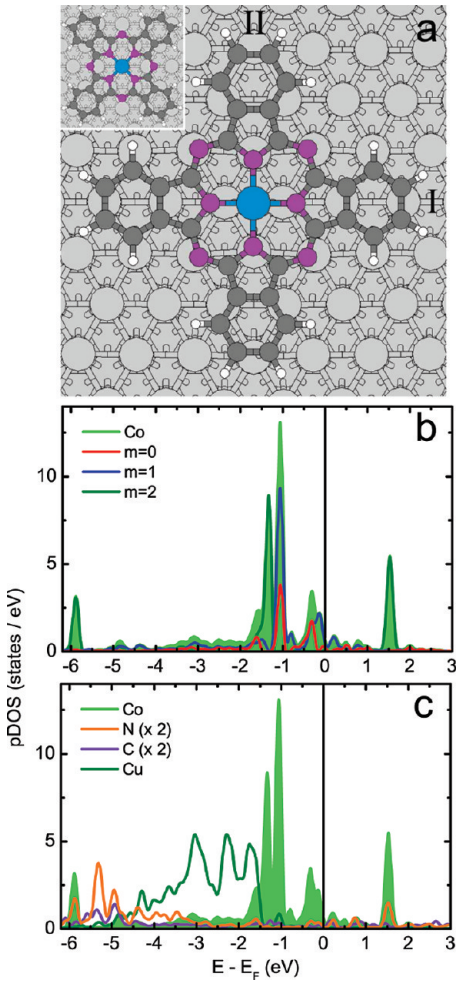

Figure 4. DFT results for CoPc on Cu(111). (a) DFT adsorption optimization for CoPc on Cu(111). Inset: Adsorption of CoPc in a top position. (b) m-Resolved contribution and total contribution of the d-states of cobalt: $m = 0$ (d_{z^2}, $d^*_{z^2}$); $|m| = 1$ (d_{xz}, d_{yz}, d^*_{xz}, d^*_{yz}); $|m| = 2$ ($d_{x^2-y^2}$, d_{xy}, $d^*_{x^2-y^2}$, d^*_{xy}). (c) pDOS of Co, N, C, and Cu atoms along axis I. The N and Cu atoms are the nearest neighbors of Co, while the C atom is taken on the pyrrole ring. The pDOS of nitrogen and carbon are scaled by a factor of 2 for clarity.

the molecule is centered between two surface atoms of copper. On the basis of Figure 2, two distinct axes running through the benzopyrrole groups of CoPc can be defined: one axis where the aromatic cycles are positioned along a close-packed direction of Cu(111) (labeled I in the inset of Figure 3), and another one along a second axis (II) forming a 90° angle with the previous one (see also Figure 3a). Since Cu(111) has a 3-fold symmetry axis, three orientations are expected for axis I and therefore CoPc. This is visible in Figure 1a and is also found in previous studies.[14,15]

Besides unveiling the adsorption of CoPc, it is also possible to visualize the molecular conductance through dI/dV maps. Compared to existing studies, these maps were acquired by keeping the tip at a constant height above a single CoPc molecule. To the best of our knowledge, constant-height maps have only been employed on rare occasions to investigate, for example, metallic nanostructures,[22,23] but never for molecules. Figure 3a−h presents maps of CoPc at selected biases. On the basis of the opening parameters of the feedback loop (see Figure 3), the center-to-center distance between the tip-apex atom and the surface atoms is close to 10 Å.[24,25] The recorded maps differ in signal localization, shape, and rotational symmetry. A quick inspection of Figure 3 is sufficient to locate the major conductance channels. If a dominant conduction channel is found over the Co atom at negative bias, confirming previous findings on other metallophthalocyanines,[6,9,26−30] our maps also unveil channels located over the benzopyrrole legs, in particular over the inner N atom nearest neighbors of Co, and over the pyrrole rings. These conduction channels are responsible for the symmetry changes of CoPc with bias. At −2.4 V, a strong conductance channel is found over one inner N atom, and the corresponding rotational symmetry of CoPc is C_1 (Figure 3a). The reason for this reduced symmetry remains unclear, but might be linked to the bulk d-states of copper present below −1.5 V (see Figure 4c). A C_2 symmetry is found for most biases, and likely reflects the two inequivalent adsorption geometries of the benzopyrrole groups along axis I and II. A C_4 symmetry is occasionally recovered at specific biases. At −0.9 V (Figure 3c), this symmetry results from the poor conductance of the

DOI: 10.1021/jz100346a | J. Phys. Chem. Lett. 2010, 1, 1517–1523

benzopyrrole legs compared to the central Co atom. At 1.6 V (Figure 3f), the map reflects a mixed contribution of the molecular states evidenced in Figure 3e and in Figure 3h.

The dI/dV maps demonstrate the prominent role played by the N atoms and the pyrrole rings in the molecular conductance of CoPc. This is an aspect of CoPc, and more generally of Pc's, that has been overlooked so far. Our data also highlight the necessity of acquiring maps of the differential conductance to properly discuss the symmetry of a molecule. Indeed, topographical images (Figure S1a in the Supporting Information) integrate the density of states from the Fermi level up to the working bias. Since intramolecular details such as those presented in Figure 3 are then washed out, their detection becomes difficult and sensitive to the tip-apex employed (Figure S2). Differential conductance maps are therefore preferable; however, as we show here, they need to be acquired at a constant height in order to avoid topography-related artifacts,[31−33] which alter the imaged conductance channels and symmetry of the molecule (Figure S1b). The contrast arising between areas of different conductance is enhanced compared to constant-current measurements; this is particularly appealing when striving for a high intramolecular resolution, and, as shown below, the comparison to the calculated data is simplified.

The identification through STM/STS of the major tunneling channels calls for a detailed simulation. The starting point of our simulations consists in determining the position of the central atom of CoPc with respect to the surface atoms, as well as the orientation of the benzopyrrole groups with respect to the compact rows. Spin-polarized calculations of the CoPc molecule on the Cu(111) substrate were carried out using density functional theory (DFT) as implemented by the PWSCF code, which is part of the QUANTUM-ESPRESSO package.[34] Ultrasoft (Vanderbilt) pseudopotentials based on local density approximation (LDA) together with a kinetic-energy cutoff of 25 Ry (Ry) for the plane wave basis set were employed (see the Supporting Information for more details and for an explanation on our choice of LDA rather than the general gradient approximation). The substrate was modeled using three layers of copper in the (111) orientation with about 22 Å vacuum to the next periodic repeated layer. Increasing the slab to four copper layers only shifted the Fermi energy by about 0.1 eV, with no appreciable change in the adsorption geometry of CoPc. The distance between the CoPc molecules of the periodic repeated cells was about 6 Å, resulting in a 249 atom model. The CoPc molecule was initially placed at 2 Å above the Cu layers. During the following adsorption optimization, only the atoms of the lowest copper layer were held fixed at the position according to the bulk values. Different starting geometries (central atom on a top, bridge, hollow position) have been checked with various orientations of the four benzopyrrole groups relative to the copper compact rows. The geometry optimization always showed that the lowest energy is obtained for a bridge position as shown in Figure 4a with a pair of benzopyrrole groups aligned with a compact row (axis I in Figure 2). The calculated adsorption is in excellent agreement with the experimental findings of Figure 2.

The adsorption of CoPc on the Cu(111) surface is driven by the reactivity of the nitrogen atoms and the benzene rings.

Table 1. Calculated DFT Total Energies (in Rydberg) Used for Determining the Adsorption Energy of CoPc on Cu(111) (Bridge Position)[a]

	component	energy [Ry]
a	CoPc/Cu(111)	−17476.932
b	Cu(111)	−16859.877
c	CoPc (vacuum)	−616.550
d	H_2Pc (vacuum)	−544.595
e	H_2Pc/Cu(111)	−17404.910
f	Co^{2+}/Cu(111)	−16933.649
g	Co (vacuum)	−73.674

[a] The Co atom has been placed above the Cu layers at the same distance as in the CoPC molecule. The positive charge of Co^{2+} was neutralized by a corresponding negative background charge in the cell.

The p_z orbitals of these atoms allow in fact for hybridization with the d_{z^2} orbitals of the copper atoms of the surface. The nitrogen atom tends to position itself above a surface atom as may be anticipated from other molecules,[16,35,36] while the benzene ring favors a flat adsorption with the center of the ring positioned in between surface atoms.[36−38] Because of the misfit between the CoPc structure and the surface, only some atoms will be in a favorable position. This misfit leads in the case of FePc/Au(111) to two coexisting adsorption geometries, with Fe either in a top position or in a bridge position.[5] In the case of CoPc/Cu(111), the adsorption optimization shows that the top and bridge positions are stable but energetically different, while the hollow position is unstable. In the top position, the nitrogen atoms are displaced relative to the copper surface atoms, and the four benzene rings are centered in a hollow site of the surface (inset of Figure 4a). The center of the benzene ring being approximately separated by 2.15 Å from the copper surface, the Co−Cu distance is forced well below the ideal Co−Cu distance (approximately 2.64 Å) and stabilizes at a distance of 2.45 Å. The benzene−copper interaction therefore produces a bended molecule (the pyrrole ring is 0.20 Å higher than the four benzene rings) with a ground state of −17477.200 Ry. On the contrary, in the bridge position all nitrogen atoms are nearly located above the copper atoms. Compared to the top position, the additional bonds to the surface save energy, and the ground state energy of CoPc is lowered by 0.3 eV. The molecule is found to be planar, with an average height above the surface plane of about 2.30 Å and with a Co−Cu distance of 2.60 Å. A similar adsorption geometry was also found for the geometry optimization of H_2Pc, which is an indication that the benzopyrrole groups govern the adsorption of CoPc as established hereafter.

The hybridization of CoPc with Cu(111) allows for an estimate of the total binding energy using DFT. The total energies of the components used are listed in Table 1. The total binding energy of CoPc on the Cu(111) surface can be obtained directly by comparing the total energy of CoPc/Cu(111) (Table 1a) with the total energy of the Cu(111) surface (Table 1b) and of the free-standing CoPc (Table 1c). Their sum yields an energy of Cu(111) + CoPc (vacuum) = −17476.427 Ry, the difference with CoPc/Cu(111) being −6.9 eV. This is the total energy gain upon adsorption. To go one step further and determine the contribution of selected parts of CoPc, we estimate the energy

DOI: 10.1021/jz100346a | J. Phys. Chem. Lett. 2010, 1, 1517–1523

of molecular fragments of CoPc. Only closed-shell parts are employed because charged fragments display a charge transfer with the surface, making the comparison to the free-standing fragment unreliable. The interaction of the Pc ligands with the surface is therefore estimated by removing Co and replacing it by two hydrogen atoms for charge neutrality, thus obtaining a H_2Pc molecule. The adsorption geometry of H_2Pc was set to the one found for CoPc (Figure 4), leaving only the H atoms to relax. Taking the Cu(111) surface (Table 1a), the free-standing H_2Pc (Table 1d) and H_2Pc on Cu(111) (Table 1e), an energy gain of about 6 eV is found for H_2Pc/Cu(111). Therefore, the total energy gain of CoPc on the Cu(111) surface can be divided in about 1 eV from Co and 6 eV from Pc. This is reasonable since the total energy of a Co^{2+} ion (zero magnetization, Table 1f) on the surface is lowered by 1.3 eV compared to the summed energies of free-standing Co (Table 1g) and Cu(111). The predicted energies do not explicitly account for van der Waals interactions. We find, however, the same adsorption for CoPc on Cu(111) when including dispersion forces as implemented in the QUANTUM-ESPRESSO package (Figure S5 of the Supporting Information), which suggests that our results should hold, at least qualitatively, in the presence of this interaction (this is also supported by the agreement found with the STM data).

The hybridization with the surface changes the electronic structure of CoPc significantly compared to the free-standing molecule. Our spin-polarized calculations show that, during the adsorption optimization, the magnetization of the central cobalt atom decreases from 1 μ_B to 0 μ_B, which is an indication of CoPc bonding to the copper atoms and charge transfer between CoPc and the surface. Figure 4b presents the projected density of states (pDOS) of the *d*-orbitals of cobalt in the bridge position. Using the isosurface plots of the molecular orbitals (MOs; Figure S3 in the Supporting Information), some insight is gained into the nature of the *d* peaks presented in the pDOS of Figure 4b. Contrary to the free-standing molecule, the $m = 0$ state, which is now filled for both spin directions, splits into a bonding state (d_{z^2}) and an antibonding state ($d^*_{z^2}$). These states can be respectively associated with the peaks falling at −1.0 eV and at −0.3 eV. As for the $|m| = 1$ states, the prominent peak falling at −1.0 eV is associated with d_{xz} and d_{yz} states, while the peak at −0.2 eV reflects d^*_{xz} and d^*_{yz} states. These $m = 0$ and $m = 1$ states provide the strong conductance channels detected in the maps over Co (Figure 3b−d). The $|m| = 2$ states have peaks at −5.9 eV ($d_{x^2-y^2}$), at −1.3 eV (d_{xy}), and at 1.5 eV ($d^*_{x^2-y^2}$). Figure 4c presents the pDOS of selected parts of CoPc. These include the cobalt atom, a neighboring nitrogen atom, a neighboring copper atom, and a C atom. Differences are found among atoms of the same species as one would expect in view of the adsorption of CoPc on the surface (Figure S4). As shown, copper possesses *d*-states located between −5 and −1 eV, therefore CoPc hybridizes with the surface in this energy range since cobalt *d*-states as well as nitrogen and carbon *p*-states are available (see the bonds in Figure S3). 4c also provides precious information on the tunneling channels observed in the d*I*/d*V* maps away from the center of CoPc. On the basis of our calculations, tunneling is expected into the p_z states of the N and C atoms over the entire energy-range investigated. The additional

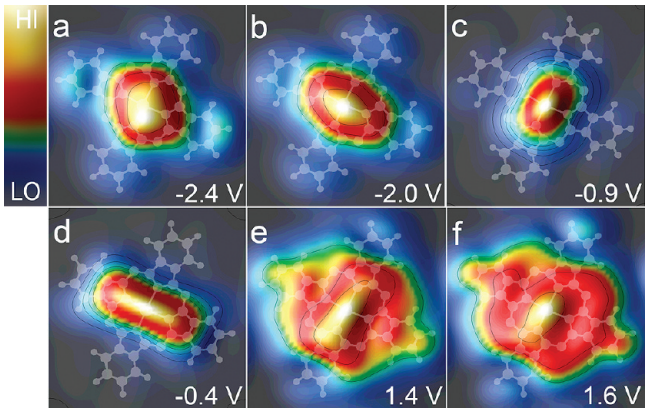

Figure 5. Calculated d*I*/d*V* maps over an isolated CoPc at selected biases: (a) −2.4 V, (b) −2.0 V, (c) −0.9 V, (d) −0.4 V, (e) 1.4 V, and (f) 1.6 V.

presence of p_x and p_y orbitals for N at 1.5 eV, however, explains the higher conductance detected over these atoms in the map of Figure 3e compared to the cobalt atom, which here only possesses $d^*_{x^2-y^2}$ orbitals (these orbitals are unfavorable to the tunneling process). At higher energies, cobalt *d*-states are no longer available, and the tunneling is governed by the N and C atoms, e.g., by the pyrrole rings (Figure 3h).

To fully compare to the experimental results of Figure 3, it is necessary to simulate the d*I*/d*V* maps. In fact, a d*I*/d*V* contrary to the pDOS depends also on how electrons tunnel between the tip and the molecule. Similar spectral features are therefore expected in the pDOS and the d*I*/d*V*, but with substantially different amplitudes. Using the adsorption optimization described above, we computed the conductance for a single molecule on Cu(111) ramping the bias from −2.5 to 2.5 V in steps of 0.1 V. A multiple scattering approach was employed,[39,40] the exchange and correlation potential being simulated by a well-tested hybrid-functional, the HSE03 functional,[41] as implemented in VASP.[42,43] The simulation directly summed up the differential contributions to avoid numerical instabilities due to numerical differentiation.[40] In the plots shown in Figure 5a−f, we evaluated the conductance in a plane parallel to the Cu(111) surface at a distance above the molecule, which coincides with the experimental tunneling conditions. Despite some differences with STS being found at positive bias, the global features of the simulated bitmaps closely mimic the experimental data, which proves that our adsorption optimization for CoPc on Cu(111) is realistic. We also find a change of symmetry with changing bias. Since a Cu monolayer was used for the hybrid-functional simulations, this indicates that the spectral features at these biases are to a large extent determined by the MOs. The changes in the rotational symmetry of Figure 3 can then be attributed essentially to a mixture of MOs produced by the molecule−metal interaction.

To summarize, we presented innovative STM techniques for characterizing a molecule on a surface. We have shown that the adsorption of a molecule can be determined by codepositing single atoms and then combining high-resolution images of the two species with a tip-assisted atom manipulation. We have also presented the first differential conductance

DOI: 10.1021/jz100346a | *J. Phys. Chem. Lett.* **2010**, *1*, 1517–1523

maps of a molecule acquired with the tip at a constant height relative to the surface and shown how they allow for a correct and clear-cut identification of the major conductance channels of the adsorbed molecule. Both techniques should be applicable to a wide variety of molecules. On the basis of the good agreement with DFT calculations, we evidenced the dual role of the benzopyrrole groups of CoPc: while they chemisorbCoPc on Cu(111), they also provide important conductance channels at positive bias, especially over the N atoms and the pyrrole rings. Finally, the constant-height conductance maps were shown to exhibit different rotational symmetries. These changes result from electronic effects as opposed to a symmetry change produced by a structural distortion of the molecule. The latter case is encountered, for example, in the adsorption of the tetrapyridyl-porphyrin molecule on Cu(111).[16]

SUPPORTING INFORMATION AVAILABLE Extra details concerning DFT calculations, as well as figures depicting theoretical and experimental results. This material is available free of charge via the Internet at http://pubs.acs.org.

AUTHOR INFORMATION

Corresponding Author:

*To whom correspondence should be addressed. E-mail: limot@ipcms.u-strasbg.fr.

ACKNOWLEDGMENT The Strasbourg authors acknowledge the Agence Nationale de la Recherche (Grant No. ANR-07-BLAN-0139, project SPINMASTER) and the International Center for Frontier Research in Chemistry (FRC) for financial support. J.K. would like to thank the European Union and the state of Saxony for financial support within the cluster of excellence Atomic Design and Defect Engineering (ADDE), and the ZIH Dresden as well for providing computational resources and assistance.

REFERENCES

(1) Reed, M. A.; Lee, T. *Molecular Nanoelectronics*; American Scientific Publishers: Stevenson Ranch, CA, 2003.

(2) Scheybal, A.; Ramsvik, T.; Bertschinger, R.; Putero, M.; Nolting, F.; Jung, T. A. Induced Magnetic Ordering in a Molecular Monolayer. *Chem. Phys. Lett.* **2005,** *411*, 214–220.

(3) Wende, H.; Bernien, M.; Luo, J.; Sorg, C.; Ponpandian, N.; Kurde, J.; Miguel, J.; Piantek, M.; Xu, X.; Eckhold, Ph.; et al. Substrate-Induced Magnetic Ordering and Switching of Iron Porphyrin Molecules. *Nat. Mater.* **2007,** *6*, 516–520.

(4) Elemans, J. A. A. W.; van Hameren, R.; Nolte, R. J. M.; Rowan, A. E Molecular Materials by Self-Assembly of Porphyrins, Phthalocyanines, and Perylenes. *Adv. Mater.* **2006,** *18*, 1251–1266.

(5) Gao, L.; Ji, W.; Hu, Y. B.; Cheng, Z. H.; Deng, Z. T.; Liu, Q.; Jiang, N.; Lin, X.; Guo, W.; Du, S. X.; et al. Site-Specific Kondo Effect at Ambient Temperatures in Iron-Based Molecules. *Phys. Rev. Lett.* **2007,** *99*, 106402–4.

(6) Iacovita, C.; Rastei, M. V.; Heinrich, B. W.; Brumme, T.; Kortus, J.; Limot, L.; Bucher, J. P. Visualizing the Spin of Individual Cobalt-Phthalocyanine Molecules. *Phys. Rev. Lett.* **2008,** *101*, 116602–4.

(7) Nazin, G. V.; Qiu, X. H.; Ho, W. Visualization and Spectroscopy of a Metal−Molecule−Metal Bridge. *Science* **2003,** *302*, 77–81.

(8) Iancu, V.; Deshpande, A.; Hla, S.-W Manipulation of the Kondo Effect via Two-Dimensional Molecular Assembly. *Phys. Rev. Lett.* **2006,** *97*, 266603–4.

(9) Takacs, A. F.; Witt, F.; Schmaus, S.; Balashov, T.; Bowen, M.; Beaurepaire, E.; Wulfhekel, W. Electron Transport through Single Phthalocyanine Molecules Studied Using Scanning Tunneling Microscopy. *Phys. Rev. B* **2008,** *78*, 233404–4.

(10) Qiu, X. H.; Nazin, G. V.; Ho, W. Mechanisms of Reversible Conformational Transitions in a Single Molecule. *Phys. Rev. Lett.* **2004,** *93*, 196806–4.

(11) Iancu, V.; Deshpande, A.; Hla, S.-W. Manipulating Kondo Temperature via Single Molecule Switching. *Nano Lett.* **2006,** *6*, 820–823.

(12) Wang, Y.; Kröger, J.; Berndt, R.; Hofer, W. A. Pushing and Pulling a Sn Ion through an Adsorbed Phthalocyanine Molecule. *J. Am. Chem. Soc.* **2009,** *131*, 3639–3643.

(13) Stadler, C.; Hansen, S.; Kröger, I.; Kumpf, C.; Umbach, E. Tuning Intermolecular Interaction in Long-Range-Ordered Submonolayer Organic Films. *Nature Phys.* **2009,** *5*, 153–158.

(14) Chang, S.-H.; Kuck, S.; Brede, J.; Lichtenstein, L.; Hoffmann, G.; Wiesendanger, R. Symmetry Reduction of Metal Phthalocyanines on Metals. *Phys. Rev. B* **2008,** *78*, 233409–4.

(15) Karacuban, H.; Lange, M.; Schaffert, J.; Weingart, O.; Wagner, T.; Möller, R. Substrate-Induced Symmetry Reduction of CuPc on Cu(111): An LT-STM Study. *Surf. Sci.* **2009,** *603*, L39–L43.

(16) Auwärter, W.; Klappenberger, F.; Weber-Bargioni, A.; Schiffrin, A.; Strunskus, T.; Wöll, C.; Pennec, Y.; Riemann, A.; Barth, J. V. Conformational Adaptation and Selective Adatom Capturing of Tetrapyridyl-Porphyrin Molecules on a Copper (111) Surface. *J. Am. Chem. Soc.* **2007,** *129*, 11279–11285.

(17) Meyer, G.; Zöphel, S.; Rieder, K.-H. Scanning Tunneling Microscopy Manipulation of Native Substrate Atoms: A New Way to Obtain Registry Information on Foreign Adsorbates. *Phys. Rev. Lett.* **1996,** *77*, 2113–2116.

(18) Repp, J.; Meyer, G.; Stojković, S. M.; Gourdon, A.; Joachim, C. Molecules on Insulating Films: Scanning-Tunneling Microscopy Imaging of Individual Molecular Orbitals. *Phys. Rev. Lett.* **2005,** *94*, 026803–4.

(19) Braun, K.-F.; Hla, S.-W. Probing the Conformation of Physisorbed Molecules at the Atomic Scale Using STM Manipulation. *Nano Lett.* **2005,** *5*, 73–76.

(20) Böhringer, M.; Schneider, W.-D.; Glöckler, K.; Umbach, E.; Berndt, R. Adsorption Site Determination of PTCDA on Ag(110) by Manipulation of Adatoms. *Surf. Sci.* **1998,** *419*, L95–L99.

(21) Stroscio, J. A.; Celotta, R. J. Controlling the Dynamics of a Single Atom in Lateral Atom Manipulation. *Science* **2004,** *306*, 242–247.

(22) Fölsch, S.; Hyldgaard, P.; Koch, R.; Ploog, K. H. Quantum Confinement in Monatomic Cu Chains on Cu(111). *Phys. Rev. Lett.* **2004,** *92*, 056803–4.

(23) Lagoute, J.; Liu, X.; Fölsch, S. Electronic Properties of Straight, Kinked, and Branched Cu/Cu(111) Quantum Wires: A Low-Temperature Scanning Tunneling Microscopy and Spectroscopy Study. *Phys. Rev. B* **2006,** *74*, 125410–8.

(24) Hofer, W. A.; Fisher, A. J. Signature of a Chemical Bond in the Conductance between Two Metal Surfaces. *Phys. Rev. Lett.* **2003,** *91*, 036803–4.

(25) Limot, L.; Kröger, J.; Berndt, R.; Garcia-Lekue, A.; Hofer, W. A. Atom Transfer and Single-Adatom Contacts. *Phys. Rev. Lett.* **2005,** *94*, 126102–4.

(26) Scudiero, L.; Hipps, K. W.; Barlow, D. E. A Self-Organized Two-Dimensional Bimolecular Structure. *J. Phys. Chem. B* **2003,** *107*, 2903–2909.

(27) Zhao, A.; Li, Q.; Chen, L.; Xiang, H.; Wang, W.; Pan, S.; Wang, B.; Xiao, X.; Yang, J.; Hou, J. G.; et al. Controlling the Kondo Effect of an AdsorbedMagnetic Ion Through Its Chemical Bonding. *Science* **2005,** *309*, 1542–1544.
(28) Takada, M.; Tada, H. Scanning Tunneling Microscopy and Spectroscopy of Phthalocyanine Molecules on Metal Surfaces. *Jpn. J. Appl. Phys.* **2005,** *44*, 5332–5335.
(29) Barlow, D. E.; Scudiero, L.; Hipps, K. W. Scanning Tunneling Microscopy Study of the Structure and Orbital Mediated Tunneling Spectra of Co(II) Phthalocyanine and Co(II) Tetraphenylporphyrin on Au(111): Mixed Composition Films. *Langmuir* **2004,** *20*, 4413–4421.
(30) Kröger, J.; Jensen, H.; Néel, N.; Berndt, R. Self-Organization of Cobalt-Phthalocyanine on a Vicinal Gold Surface Revealed by Scanning Tunnelling Microscopy. *Surf. Sci.* **2007,** *601*, 4180–4184.
(31) Stroscio, J. A.; Feenstra, R. M. *Scanning Tunneling Microscopy*; Academic: New York, 1993; Vol. 27.
(32) Ukraintsev, V. A. Data Evaluation Technique for Electron-Tunneling Spectroscopy. *Phys. Rev. B* **1996,** *53*, 11176–11185.
(33) Ziegler, M.; Néel, N.; Sperl, A.; Kröger, J.; Berndt, R. Local Density of States from Constant Current Tunneling Spectra. *Phys. Rev. B* **2009,** *80*, 125402–6.
(34) PWscf is part of the Quantum-ESPRESSO package distributed by Baroni, S.; A. Dal Corso, S. de Gironcoli, Giannozzi, P.; Cavazzoni, C.; Ballabio, G.; Scandolo, S.; Chiarotti, G.; Focher, P.; Pasquarello, A.; Laasonen, K.; Trave, A.; Car, R.; N.Marzari, Kokalj, A.; , http://www.pwscf.org/.
(35) Bocquet, M.-L.; Lesnard, H.; Lorente, N. Inelastic Spectroscopy Identification of STM -Induced Benzene Dehydrogenation. *Phys. Rev. Lett.* **2006,** *96*, 096101–4.
(36) Lesnard, H.; Lorente, N.; Bocquet, M.-L. Theoretical Study of Benzene and Pyridine STM Induced Reactions on Copper Surfaces. *J. Phys.: Condens. Matter* **2008,** *20*, 224012–7.
(37) Lagoute, J.; Kanisawa, K.; Fölsch, S. Manipulation and Adsorption-Site Mapping of Single Pentacene Molecules on Cu(111). *Phys. Rev. B* **2004,** *70*, 245415–6.
(38) Lagoute, J.; Fölsch, S. Interaction of Single Pentacene Molecules with Monatomic Cu/Cu(111) Quantum Wires. *J. Vac. Sci. Technol. B* **2005,** *23*, 1726–1731.
(39) Palotas, K.; Hofer, W. A. Multiple Scattering in a Vacuum Barrier Obtained from Real-Space Wavefunctions. *J. Phys.: Condens. Matter* **2005,** *17*, 2705–2713.
(40) Hofer, W. A.; Garcia-Lekue, A. Differential Tunneling Spectroscopy Simulations: Imaging Surface States. *Phys. Rev. B* **2005,** *71*, 085401–8.
(41) Heyd, J.; Scuseria, G. E.; Ernzerhof, M. Hybrid functionals based on a screened Coulomb potential. *J. Chem. Phys.* **2003,** *118*, 8207–8215.
(42) Kresse, G.; Hafner, J. Ab initio molecular dynamics for liquid metals. *Phys. Rev. B* **1993,** *47*, 558–561.
(43) Kresse, G.; Joubert, D. From Ultrasoft Pseudopotentials to the Projector Augmented-Wave Method. *Phys. Rev. B* **1999,** *59*, 1758–1775.

DOI: 10.1021/jz100346a | *J. Phys. Chem. Lett.* **2010,** *1*, 1517–1523